

Demonstration of classical chaotic scattering

C Bercovich†, U Smilansky† and G P Farmelo‡

† Department of Physics, Weizmann Institute of Science, 76100 Rehovot, Israel

‡ Physics Department, The Open University, Walton Hall, Milton Keynes, MK7 6AA, UK

Received 7 September 1990

Abstract. It is possible to demonstrate classical chaotic scattering by scattering laser light from symmetrically positioned circular discs. The apparatus is described in detail and we explain how the results illustrate several of the principles of chaotic scattering. In particular, we use this phenomenon to introduce in a natural way the abstract concepts of the Cantor set and its fractal dimension.

Résumé. Il est possible de démontrer la diffusion chaotique classique en observant la diffusion du faisceau d'un laser de quelques disques symétriquement posés. L'expérience est décrite en détail aussi que les relations entre les résultats expérimentaux et plusieurs principes de la diffusion chaotique. En particulier, on peut se servir de ce phénomène afin d'expliquer, d'une façon naturelle, le concept abstrait de l'ensemble de Cantor et sa dimension fractale.

1. Introduction

The concept of a chaotic system is now very familiar—indeed, it is now known that chaotic behaviour in classical systems is the rule rather than the exception. By definition, the time development of a chaotic system is exponentially sensitive to its initial conditions in phase space. This sensitivity implies that although the system is deterministic, in the sense that its time development is determined by well defined equations of motion, one cannot in practice predict the state of the system over long times. This gives rise to the crucial—and, at first sight, paradoxical—idea that the behaviour of a classical system can be both deterministic and unpredictable. (For reviews of classical chaos, see Berry (1983) and Ford (1988).)

This phenomenon was originally observed in systems that are *bounded* or, in other words, *confined*. However, it has become clear that chaos appears also in scattering problems, in which the dynamics is *unbounded* (Jung 1986, Noid *et al* 1986, Petit and Hénon 1986, Eckhardt 1988, Hénon 1989, Blümel and Smilansky 1990). The characteristic features of chaotic scattering are strikingly manifest in the behaviour of the associated reaction function, which gives the dependence of the parameters that specify the outcome of the collision in terms of those that characterize the incoming channel. When the scattering is chaotic, this function fluctuates wildly: there is an infinite number of points in whose vicinity a small variation in the initial conditions induces arbitrarily

large changes in the outcome of the scattering process. (A typical example of a reaction function is shown and described later, in figure 2). Further study shows that the singular points of a reaction function are associated with trajectories that are trapped forever in the region in which the interaction between the scattered particle and the scatterer takes place. The closer a scattering trajectory is to a trapped trajectory, the longer it will spend in the interaction region, and the more severely affected it will be by the chaoticity (instability) of the trapped unstable orbits.

The process of identifying the trapped trajectories and the corresponding singularities in the reaction function brings us close to the theory of 'strange sets' of the type first introduced by Cantor in his investigations of the theory of the continuum. These sets were long considered as purely theoretical concepts. However, recent studies have shown that Cantor sets appear very naturally in chaotic dynamics, and they determine the behaviour of physical systems (Mandelbrot 1982, Gleick 1987, Kaye 1989). Chaotic scattering is probably the simplest physical system in which these sets emerge and play an important role. We use this to our advantage here, as a means of introducing Cantor sets and the surprising concept of a non-integer dimension.

A particularly simple example of a chaotic system is provided by a point particle that is elastically scattered in a plane from three non-colinear hard circular discs (figure 1). This system has proved to be a very fruitful area of study—not only is it amenable

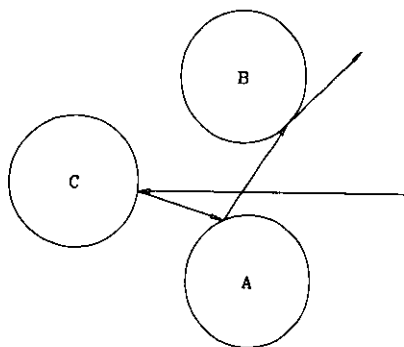


Figure 1. The type of scattering studied in this paper. The centres of the three circular discs are located on the corners of an equilateral triangle. The particles are scattered by the discs, in a plane.

to classical, semi-classical and quantum mechanical analysis, it also forms the basis of a model of unimolecular fragmentation (Eckhardt 1987, Gaspard and Rice 1989).

For the three-disc system, the reaction function we considered is the difference between the outgoing angle of a scattered particle and the incoming angle, as a function of the initial impact parameter b . Hence, in this case, the reaction function is a *deflection function*. Figure 2(a) shows this function, and its complex structure is emphasized by showing magnified details of this function in parts (b) and (c) of figure 2, in which there is the same oscillatory pattern as the one in figure 2(a). If figure 2(c) were to be magnified, the same structure would be observed on a yet smaller scale, and so on *ad infinitum*. Chaotic reaction functions are in general characterized by this self-similar complexity, that is, by their fractal structure.

This paper describes how the three-disc configuration can be used experimentally to demonstrate several of the most important features of chaotic scattering. We begin in section 2 by reviewing briefly the dynamics of the system, drawing attention to the points that can easily be illustrated with the apparatus. In section 3, we describe in detail how the three-disc model can be set up in a laboratory with the aid of a laser and some easily obtained materials and equipment. We also point out the features of chaotic scattering that can be demonstrated using the apparatus. Finally, in section 4, we present a brief summary.

2. The three-disc configuration and the associated Cantor set

The model that we shall consider consists of three circular discs whose centres are located on the corners of an equilateral triangle (figure 1). The particles that enter the scattering region are assumed to be elasti-

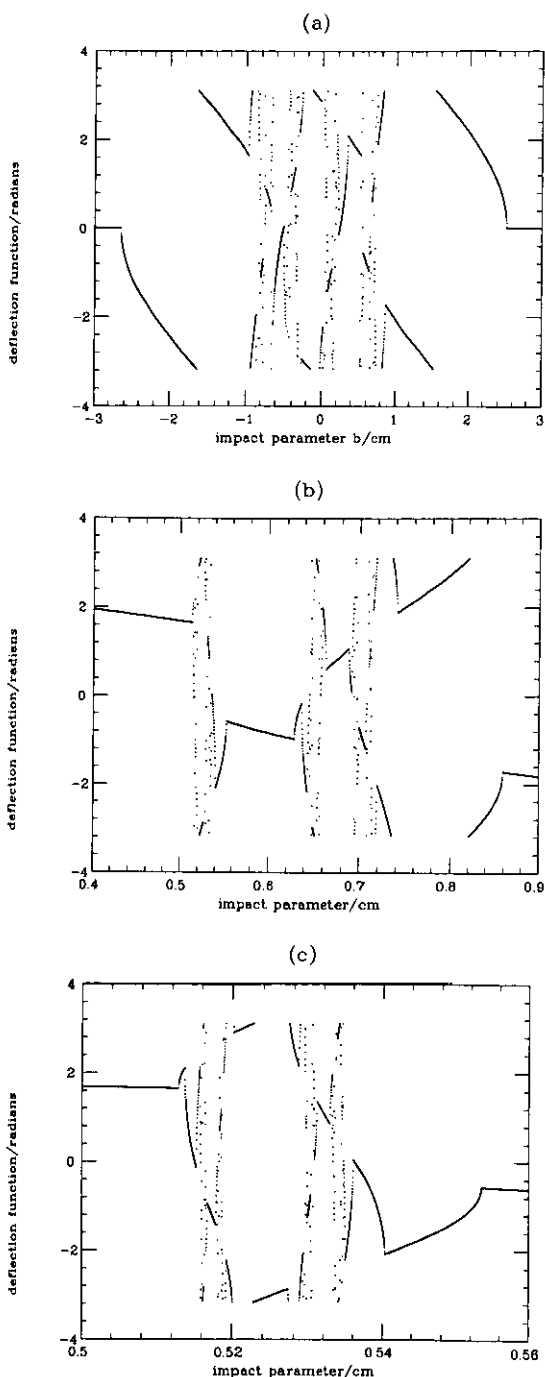


Figure 2. The deflection function associated with the scattering of particles from the configuration shown in figure 1. Zero impact parameter $b = 0$ corresponds to paths that are initially directed towards the centre of the apparatus, equidistant from the centres of the three discs. The deflection function has a fractal structure—the same structure is manifest on decreasing scales ((a), (b) and (c)).

cally scattered in a plane by the surfaces of the discs, which we shall label A, B and C. It is convenient to use symbolic dynamics to label each scattered particle's trajectory, by specifying the order in which it collides with the discs. For example, if a particle collides first with C, then with A, and then finally with B before it leaves the scattering region, the trajectory is labelled CAB (figure 1). Obviously, the 'length' of a trajectory's label can consist of any number of the symbols A, B and C between one and infinity, and no two consecutive symbols in the label can be the same.

An alternative assignment of symbols to trajectories can be given by using as a label the sense in which the particle propagates from one disc to the next: if the propagation is clockwise, it is denoted by R, for right, and if the propagation is counterclockwise it is denoted by L, for left. In this language, trajectories are coded by strings composed of two symbols, and there are no restrictions on the allowed sequences. Thus, we obtain a 'binary code' that is essentially the same as the one used to represent real numbers in a binary basis in a computer. However, our codes are not limited to a finite number of digits. (The initial disc from which scattering occurs cannot be specified by the binary code. However, because of the symmetry of the problem, this is completely immaterial.)

It is instructive to examine the conditions in which a particle undergoes an increasing minimum number of collisions with the disc—at least one, at least two, at least three etc—in order to study the progression towards the extreme condition of permanent confinement, the characteristic feature of chaotic scattering. For the sake of definiteness, we shall consider incoming trajectories for which the angle of incidence is fixed.

Let us consider the intervals of the incoming impact parameter for which a particle will collide a specified minimum number of times with the discs. First, we shall define Δb_A to be the interval in impact parameter for which the incident particle collides initially with disc A. The total impact parameter interval Δb_1 for the first generation of scatterings is defined as the sum of the impact parameter intervals for at least one scattering: $\Delta b_1 \equiv \Delta b_A + \Delta b_B + \Delta b_C$.

The total impact parameter Δb_2 for the second generation of scatterings is defined analogously as the interval in impact parameter for which the incoming particle collides at least twice. If Δb_{AB} is the interval for which the first two scatterings are from A and then B, then $\Delta b_2 \equiv \Delta b_{AB} + \Delta b_{AC} + \Delta b_{BA} + \Delta b_{BC} + \Delta b_{CA} + \Delta b_{CB}$ (note that the set that corresponds to at least two collisions is a subset of the set corresponding to at least one collision, $\Delta b_2 \subset \Delta b_1$). Similarly, the third generation interval is given by $\Delta b_3 \equiv \Delta b_{ABA} + \Delta b_{ABC} + \Delta b_{ACA} + \Delta b_{ACB} + \Delta b_{BAC} + \Delta b_{BAB} + \Delta b_{BCA} + \Delta b_{BCB} + \Delta b_{CAB} + \Delta b_{CAC} + \Delta b_{CBA} + \Delta b_{CBC}$ ($\Delta b_3 \subset \Delta b_2$). It is easy to see that this procedure can be used to find Δb_n for an arbitrary generation number and hence to show inductively that

$\Delta b_n \subset \Delta b_{n-1}$ and that the number of intervals in the n th generation is $3(2^{n-1})$.

The ratio $\Delta b_{n+1}/\Delta b_n$ between the lengths of successive sets can be interpreted as the probability that the particle, having been scattered n times, does not escape the scatterer before being reflected once more from a disc. This ratio is expected to approach a constant g as $n \rightarrow \infty$ because after many collisions the particle loses all memory of its past, and its chance of escaping depends on average only on the width of the 'escape channels' between the discs, relative to the circumference of the enclosure between the three discs. We can summarize the situation by saying that, as the generation number n increases, the number of subintervals *proliferates* as 2^n while the length of each of them *decreases* as $(g/2)^n$. In the limit, the intervals converge to points. Thus, intervals of impact parameter become narrower as the corresponding scattering trajectories spend longer times in the interaction region. The points to which these intervals converge define the trajectories that spend arbitrarily long times in the interaction region—these are the trapped orbits.

Sets of points that are generated by this type of limiting process were originally introduced by Cantor and they bear his name. The canonical example of a Cantor set is constructed in the way illustrated in figure 3. One starts from an interval of unit length and divides it into three equal intervals, of which the middle one is discarded. One attaches the letter L to the left interval and the letter R to the right interval. Each subinterval is again divided into three equal intervals and the middle ones are again discarded. There are now four intervals, each of length $\frac{1}{3}$, which are denoted as LL, LR, RL and RR. This procedure is repeated successively and it is easily seen that at each generation the number of intervals *increases* by a factor of 2, while the length of each subinterval *decreases* by a factor of 3. After n divisions, each interval is labelled by a symbol which is n letters long, composed of the letters L and R. When this process is continued *ad infinitum* one obtains a set of points—the Cantor set. The similarity between the canonical Cantor set and the set we defined using our scattering experiment is now evident because both are encoded by a binary code. The difference is that, in the case of scattering, the removal of the middle interval is effected by the escape of trajectories in the scattering Cantor set.

Cantor sets defy our intuition: on the one hand, there is a *one-to-one* correspondence between the points in the Cantor set and the points in the interval $[0, 1]$. On the other hand, the total 'length' of the Cantor set is *zero* since at each stage, the total length of all the intervals is $(2/3)^n$, so in the limit $n \rightarrow \infty$, the 'length' vanishes. Thus, the unit interval and the Cantor set have the same 'number' of points but completely different lengths. A slightly more detailed comparison between the canonical Cantor set and the scattering Cantor set makes matters even more perplexing. The points have the same codes in both sets,

and therefore they have the same 'number'. However, their lengths have a ratio that is not unity for most values of g ! This counter-intuitive phenomenon shows that in order to deal with such sets, one has to sharpen the definitions of 'length' or 'dimensionality'. Otherwise, intuition can lead one astray.

A quantitative measure for the 'length' of a Cantor set can be given in terms of the set's 'fractal dimension', a concept that can be explained quite easily. First, we need to look closely at the definition of a dimension of an object, so that we can generalize the concept and apply it to Cantor sets. In order to motivate the idea of dimension, consider the following thought experiment: draw a line in the plane that encloses a certain area; take coins of a given radius r and count the number $N_{\text{area}}(r)$ that are needed to cover the area, and count the number of coins $N_{\text{line}}(r)$ that are necessary to cover only the line; repeat the experiment several times, each time with coins of a smaller radius. If the functions $N_{\text{area}}(r)$ and $N_{\text{line}}(r)$ are now plotted as a function of r , it is found that the two functions diverge as $r \rightarrow 0$, but at different rates. Both functions can be fitted by an expression of the form $N_0 r^{-d}$, here N_0 is a constant and d takes the value $d = 1$ for the function N_{line} and $d = 2$ for N_{area} . The 'dimension' of an object is simply the *exponent* that determines the number of coins needed to cover the object when the size of the unit of length used (r in our case) approaches zero:

$$d = -\lim_{r \rightarrow 0} [\ln N(r)/\ln(r)] \tag{1}$$

Using equation (1), we can now find the dimension of a Cantor set. The intervals one has in the n th generation certainly cover the Cantor set. Hence, if discs with the size $(g/2)^n$ were used, $3(2^{n-1})$ discs would be needed to cover the scattering Cantor set. Hence, by using equation (1) a *non-integer* value for the dimension d is obtained:

$$d = \ln(2)/[|\ln(g)| + \ln(2)]. \tag{2}$$

This shows that the dimension of the canonical Cantor set is $\ln(2)/\ln(3)$, as it must be, according to its definition (figure 3).

We shall now show how the fractional dimension of equation (2) can be related to physically meaningful quantities. Because g measures the probability that the particle will be scattered once more, after the n th scattering (for large n), the probability that the particle will be scattered n times can be expressed as $e^{-\gamma n}$, where $\gamma = |\ln(g)|$. Hence, γ is the inverse 'lifetime' of the ensemble of scattering trajectories: it takes $1/\gamma$

collisions to reduce the number of trajectories within the interaction region by a factor $1/e$. Another important quantity that appears here is the factor $g/2$, which measures the rate of shrinkage of the width of an impact parameter interval. This exponential thinning of each interval reflects the lack of stability of the scattering dynamics. At the same time that the contraction of the intervals occurs, the uncertainty in the conjugate variable (the angle in this case) increases. Thus $\lambda = |\ln(g)| + \ln(2)$ characterizes the exponential sensitivity of the angle to 'infinitesimal' changes in the initial conditions: λ is the Lyapunov exponent in this case. If all these quantities are substituted into the expression for d (equation (2)), it is found that

$$\gamma = (1 - d)\lambda. \tag{3}$$

This relation is a characteristic feature of chaotic scattering, and is by no means true only for our simple problem. It reflects the intimate connection between dynamical instability, the fractal dimensionality and the physically observable 'lifetime' of the scattering ensemble.

In the experiment that we describe here, the parameters γ , d and λ can in principle be measured. In particular, we shall demonstrate the proliferation of subintervals in b_n , and determine γ by measuring the ratios $\Delta b_{n+1}/\Delta b_n$. However, because we are dealing with a chaotic system, any error in specifying an accurate value in the value of the impact parameter increases exponentially when one wants to measure effects that correspond to long dwell times in the chaotic domain. For this reason, we shall be able to measure only the intervals Δb_1 , Δb_2 and Δb_3 . If the apparatus were to be replaced by a computer simulation, n could be increased to 15 or to 30, depending on whether single or double precision is used and on the amount of CPU time that is available. This is an important illustration of the concept of 'deterministic unpredictability' which we mentioned in the introduction. Our measurements will be adversely affected by transients that are always present when one is not well into the domain of large n . We shall take this into account by comparing our experimental results with the more precise computer simulations.

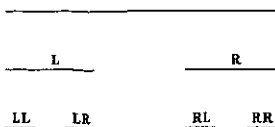
3. Demonstration of chaotic scattering effects

3.1. The apparatus

The apparatus described here makes it possible to observe the scattering from three circular discs configured as in figure 1. The observations are made possible by scattering laser light from cylinders that are covered with a highly reflective coating—the elastically scattered particles are, in this case, photons.

A photograph of the apparatus is given in figure 4.

Figure 3. The first stages in the generation of a Cantor set from a straight line.



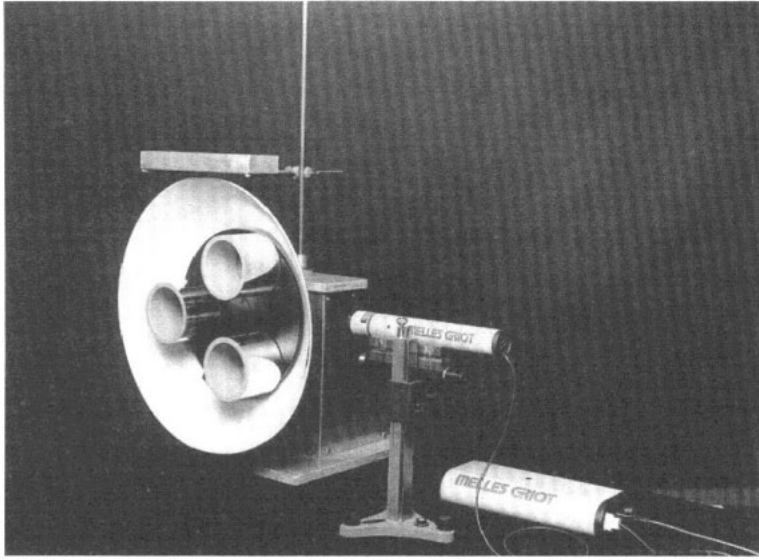


Figure 4. Photograph of the apparatus.

The outer diameter of each of the cylinders is 12 cm, and their centres are accurately positioned on the corners of an equilateral triangle that has sides of length 19 cm. These dimensions are not critical. However, it is important for quantitative work that the apparatus is well engineered, so that the discs are accurately positioned, with precisely circular cross sections. We found that, for the purposes of demonstration, it is convenient to use cylinders that have a height of approximately 9 cm, although once again this dimension is not critical.

The source of light is an ordinary helium–neon laser of the type found in any optics laboratory. The laser is mounted on a travelling microscope that enables the vertical height of the beam to be finely adjusted (to within about 0.1 mm). This facilitates the measurements of the impact parameter intervals for successive generations of scattering, and we shall discuss these data shortly.

The light is scattered by the rigidly mounted cylinders, which are coated with an extremely smooth and highly reflective coating. For this purpose, we used aluminized Mylar, an inexpensive and readily available material, commonly used in cryogenic experiments. It is not advisable to use an inferior substitute such as aluminium foil because the surface of this material tends to be uneven and crinkly after it has been attached to the surface of the cylinder. It is also important to protect the reflecting surface of the Mylar from damage and from soiling by dirt, dust, fingerprints etc. This protection can be readily achieved by wrapping each cylinder with a tightly fitting paper cover that is removed only during experiments.

The cylinders are mounted on a rigid plane surface that can be rotated by up to 120° (by symmetry, any further angular adjustability is superfluous). The angle of rotation is recorded on a linear scale that is fixed on the outside of the rotating surface. The scattered beam is detected on a fixed screen that surrounds the mounted cylinders in the vertical plane. It is, of course, necessary to cut a vertical slit in this screen in order to allow the beam to enter the apparatus and to allow the height of the beam to be adjusted. In our apparatus, the slit has a vertical height of 15 cm and a width of 5 cm.

For an ordinary helium–neon laser with a modest beam intensity, it is often difficult to observe the path of the scattered beam, even in a darkened room. One solution to this problem is to pour liquid air into a metallic container that is fixed above the apparatus (figure 4); when the liquid evaporates, the falling vapour enables the path of the beam to be identified after a maximum of three scatterings. This method has the disadvantage that it is difficult to maintain the density of the vapour at a satisfactory level. A more effective solution is to blow into the path of the scattered beam a supply of smoke which can be generated conveniently, if unhealthily, by burning a cigarette.

3.2. Observation of chaotic scattering effects

Before the apparatus is used, it is important to ensure that it is securely fixed to the work surface and aligned in such a way that the scattering takes place in a plane. This alignment can be made easily by reflecting the laser light by slightly less and by slightly more than

180° from the discs and by then checking that the reflected beam is in the same plane as the incident beam.

The most striking effect that can be demonstrated using the apparatus is the unboundedness of the scattering for certain scattering angles. At most angles of incidence, the scattering is regular and so a point is detected on the screen, just as should be expected intuitively. However, when the beam grazes one or more of the cylinders the scattering becomes unstable and *the whole screen is illuminated* (apart, of course, from areas that are in the shadows of the cylinders). Under these conditions, the scattering is very sensitive to small perturbations in the dimensions of the scatterer: if the beam is slightly deflected by putting a tiny object in its path, the image on the screen changes markedly.

Because the laser beam has a narrow but non-zero width, the incident trajectories have initial conditions that are close together in phase space. When the system is chaotic, these nearby trajectories diverge rapidly from one another and their rate of separation is measured by the system's Lyapunov exponent. It is possible in principle to measure this exponent by measuring the width of the beam after each successive scattering. Such measurements allow one to demonstrate convincingly that, under chaotic conditions, the Lyapunov exponent is non-zero. A quantitative determination of the exponent is precluded by the difficulty of measuring the width of the beam after the second scattering and by the resolution of the apparatus, which we found would permit the unambiguous identi-

fication of scattering only up to the third generation. The finite resolution of the apparatus limits the degree of detail that one can observe in the fractal deflection function (figure 2).

Using the present apparatus, it is possible to study qualitatively the exponential proliferation of the segments that make up the *n*th generation of scattering. The definition of the first generation interval Δb_1 requires some care as it is important to exclude scattering that is not characteristic of the long-time behaviour of the system. For this reason, any trajectory that has an impact parameter below the centre of disc A or above that of disc B (figure 1) must be excluded from this generation. It is straightforward to identify experimentally this first generation and the second, but difficulties arise when observing the third, owing to the small widths of most of the scattered beams in this generation (the same problem would of course occur for higher generations if they were measurable). This problem makes it necessary to decide on a criterion to determine the beginning and end of each interval; for the *n*th generation, we took the starting point of the interval to be the point at which the first part of the beam is deflected at least *n* times, and the corresponding end point as the point at which the last part of the beam is deflected at least *n* times.

In table 1, our experimental results are compared with the results of a computer simulation for the configuration in which the line connecting the centre of disc A to the centre of disc B subtends, in the upper right-hand quadrant, an angle of 92° (figure 1). From these data, we calculated the impact parameter inter-

Table 1. Impact parameter intervals.†

Δb_A		Δb_B		Δb_C			
6.00		6.73		6.00			
(6.00)		(6.99)		(6.00)			
Δb_{AB}	Δb_{AC}	Δb_{BA}	Δb_{BC}	Δb_{CA}	Δb_{CB}		
0.30	1.46	2.31	2.29	1.47	0.30		
(0.18)	(1.31)	(2.20)	(2.16)	(1.38)	(0.24)		
Δb_{ABA}	Δb_{ABC}	Δb_{BAB}	Δb_{BAC}	Δb_{CAB}	Δb_{CAC}	Δb_{CBA}	Δb_{CBC}
0.06	0.13	0.62	0.53	0.19	0.40	0.08	0.08
(0.02)	(0.06)	(0.53)	(0.38)	(0.16)	(0.38)	(0.08)	(0.04)
Δb_{ACA}	Δb_{ACB}	Δb_{BCA}	Δb_{BCB}				
0.40	0.21	0.49	0.58				
(0.30)	(0.14)	(0.38)	(0.52)				

† For the configuration in figure 1 (details are given in the text). The first number given in each case is the experimental measurement of the interval in centimetres (for each of these measurements, the uncertainty is ± 0.04 cm). The bracketed number below is the interval calculated in the computer simulation (for each of these data, the uncertainty is negligible).

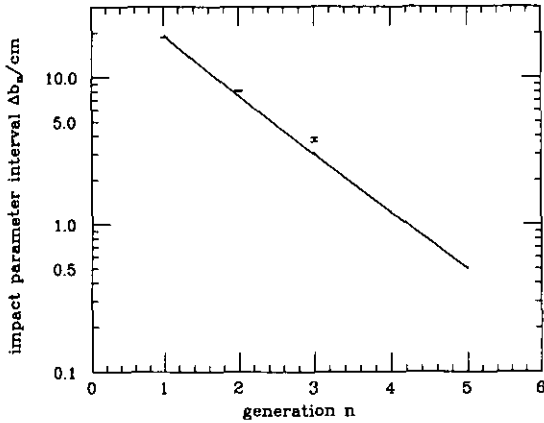


Figure 5. Comparison between the experimental measurements of Δb_n and the results of our computer simulation. The (small) error bars associated with the experimental points are shown; those associated with the simulation are not, because they are negligibly small.

vals Δb_n for $n = 1, 2$ and 3 : the results are plotted (with error bars) in figure 5 where the data are compared with the results of the computer simulation, shown by the full line. The agreement between the experimental result, $\Delta b_2/\Delta b_1 \approx \Delta b_3/\Delta b_2 \approx 0.4$, and the result of the computer simulation is good; the discrepancy is probably due mainly to imprecisions in the construction of the apparatus and to the difficulties involved in taking the data for the third generation.

4. Summary

Demonstrations of chaotic *bounded* systems are now relatively common (see, for example, Núñez Yépez *et al* (1989) and references therein). Our innovation in this paper has been to present a simple experimental demonstration of classically chaotic scattering. The system that we have studied—the elastic scattering of particles by three circular discs, arranged as in figure 1—has enabled the qualitative illustration of several key features of chaotic scattering, notably: the unboundedness of the scattering; the sensitivity to the initial scattering conditions; the non-zero Lyapunov exponent. It is also possible to begin to study quantitatively the exponential proliferation of the segments that make up the n th generation of scattering, although such investigations are limited by the resolution that is possible using the simple equipment that we have used. This experiment can also be used

to introduce naturally the concepts of a Cantor set and fractional dimensions, and to demonstrate their relevance to physical situations.

The apparatus was designed to give pedagogic insights into the nature of classical chaotic scattering. However, it should be possible to develop the design, for example by using a laser with a finer beam width and a higher beam intensity, in order to increase the resolution. This would in turn improve the ability of the apparatus to make quantitative measurements of the chaotic scattering process.

Acknowledgments

For their help in constructing the first two prototypes of the apparatus, we should like to thank Reuven Anati of the Weizmann Institute and Martin Jarvis, Barrie Jones and Alan Cooper of The Open University. This research was supported in part by grants from the German-Israeli Foundation for Scientific Research and Development and the US-Israel Binational Science Foundation. One of us (GPF) would like to thank his colleagues at Northeastern University, especially Professor Jorge José, for their hospitality while part of this work was completed.

References

- Berry M V 1983 *Chaotic Behaviour of Deterministic Systems, Les Houches Lectures XXXVI* ed G Iooss, R H G Helleman and R Stora (Amsterdam: North-Holland)
- Blümel R and Smilansky U 1989 *Phys. Blat.* **45** 379–81
- Eckhardt B. 1987 *J. Phys. A: Math. Gen.* **20** 5971–9
—1988 *Physica D* **33** 89–98
- Ford J 1988 *The New Physics* ed P Davies (Cambridge: Cambridge University Press) pp 348–72
- Gaspard P and Rice S A 1989 *J. Chem. Phys.* **90** 2225–41, 2242–54, 2255–62.
- Gleick J 1987 *Chaos: Making a New Science* (Harmondsworth: Penguin)
- Hénon M 1989 *La Recherche* **20** 491–8
- Jung C 1986 *J. Phys. A: Math. Gen.* **19** 1345–53
- Kaye B H 1989 *A Random Walk Through Fractal Dimensions* (VCH)
- Mandelbrot B B 1982 *The Fractal Geometry of Nature* (San Francisco, CA: Freeman)
- Noid D W, Gray S and Rice S A 1986 *J. Chem. Phys.* **84** 2649–52
- Núñez Yépez H N, Salas Brito A L, Vargas C A and Vicente L A 1989 *Eur. J. Phys.* **10** 99–105
- Petit J M and Hénon M 1986 *Icarus* **66** 536–55
- Smilansky U 1990 *Chaos and Quantum Physics, Les Houches Lectures* ed A Voros, M Gianonni and O Bohigas (Amsterdam: North-Holland)